

Supporting Information

Delineating the Enhanced Efficiency of Carbon Nanomaterials Included Hierarchical Architecture of Photoanode of Dye Sensitized Solar Cells

Venkatesan Srinivasan^a, Jagadeeswari Sivanadanam^{b*}, Kothandaraman Ramanujam^b, Mariadoss Asha Jhonsi^{a*}

^aDepartment of Chemistry, B. S. Abdur Rahman Crescent Institute of Science and Technology,
Vandalur, Chennai – 600 048, Tamil Nadu, India.

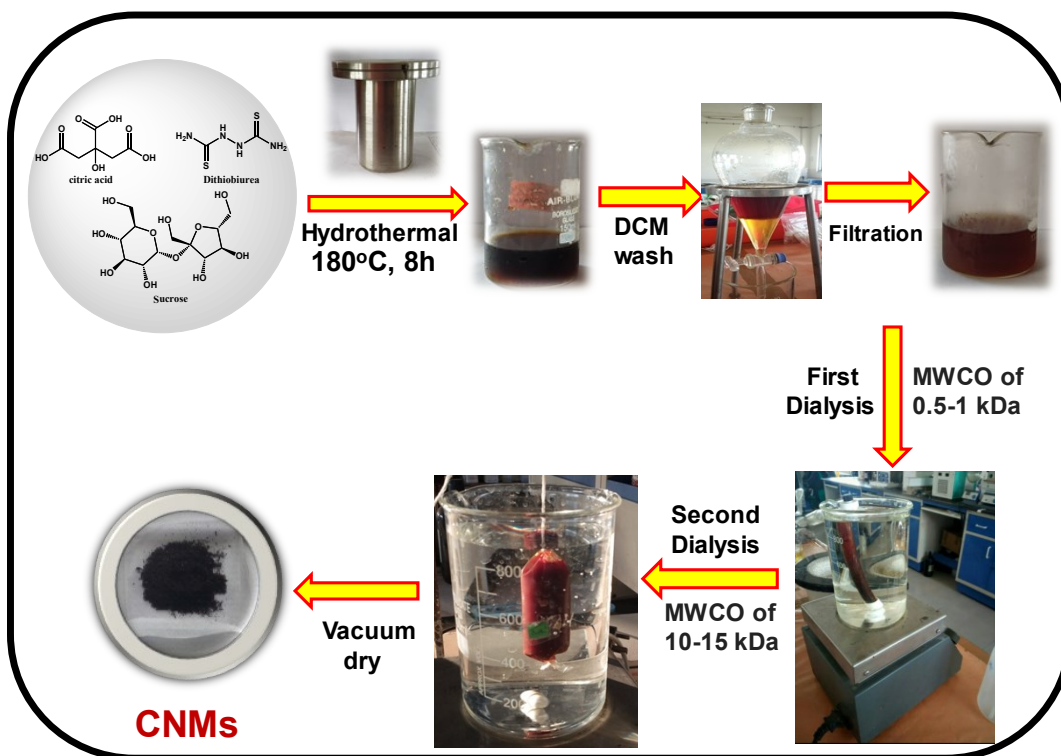
^bDepartment of Chemistry, Indian Institute of Technology Madras, Chennai –36, Tamil Nadu,
India.

E-mail: jhonsiasha@gmail.com (Mariadoss Asha Jhonsi);
Jagadhi333@gmail.com (Sivanadanam Jagadeeswari)

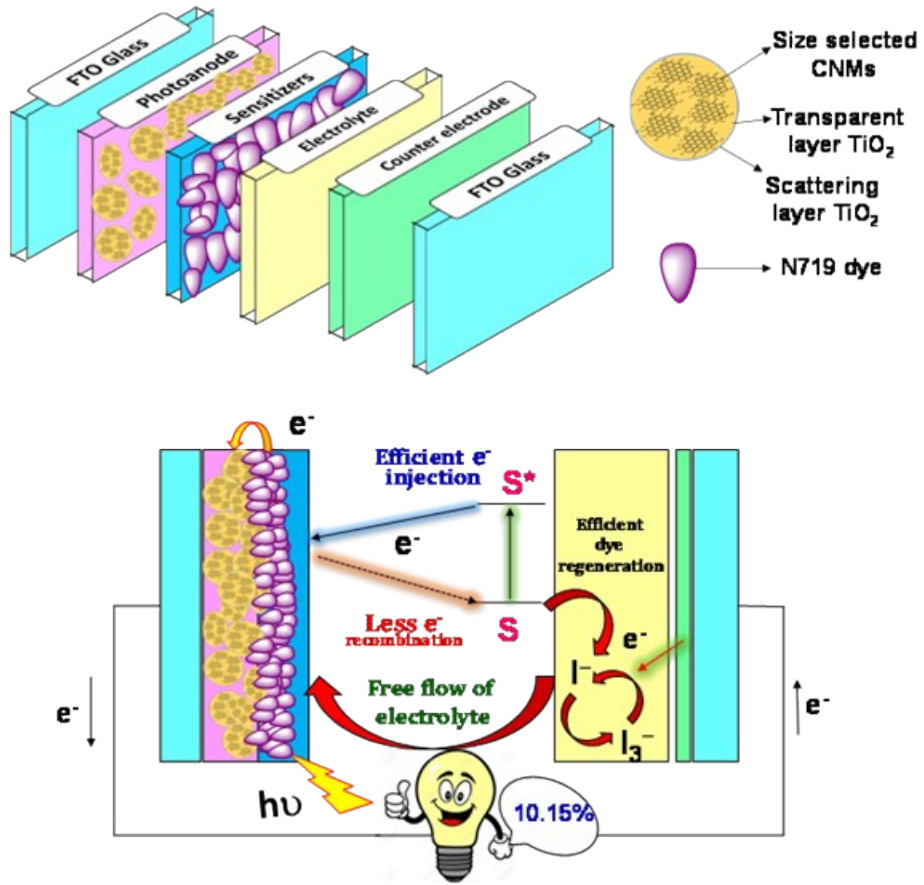
Experimental details

Materials and Methods

The details of the chemicals used for synthesis of carbon nanomaterials and solar cell device fabrication are given below. The starting materials (citric acid, sucrose and dithiobiurea), iodine and lithium iodide (LiI) were purchased from Sigma Aldrich. All solvents were of spectro-metric grade and were used without further purification. Titania (TiO_2) paste (18NR-T), Fluorine-doped SnO_2 (FTO, $15\Omega\text{cm}^{-2}$ and 2.2 mm) conducting glass (MS001695-10) and hotmelt sealing agent (MS004610-10, 30 mm thick thermoplastic film) were purchased from Dyesol Ltd., Australia.



Scheme S1: Various stages of synthesis of carbonaceous nanomaterials (CNMs).



Scheme S2: Schematic Representation of fabricated photoanode and working mechanism of the device.

Table S1: Elemental details from HR-SEM-EDS analysis

Sample	C %	H%	N%	S%	O%	Ti%
CNMs	29.31	-	11.08	04.37	55.24	-
TiO ₂	-	-	-	-	58.05	41.95
TiO ₂ with 0.5wt.% CNMs	8.09	-	0.00	0.81	52.36	38.74

The elemental composition values are given in wt.-%.

Table S2: Elemental composition of CNMs and TiO₂ loaded with 0.5 wt.% of CNMs obtained using CHNOS elemental analysis

Sample code	%C	%H	%N	%S	%O
CNMs	40±5	4.7±0.34	10.7±0.49	9.99±0.43	36.6±0.36
0.5 wt.% CNMs-TiO ₂	0.1322±0.001	0.18±0.004	0.006±0.001	0.07±0.109	4.2±0.12

The given elemental values are in at.%. (in CNM-TiO₂, quantity of S and N appear insignificant)

Table S3: Data from BET-adsorption isotherm analysis

Sample	Surface area, m ² /g	Pore volume, cm ³ /g	Pore size, Å°
CNMs	2.32 ± 0.0588	-	-
TiO ₂	64.76 ± 0.2747	0.3229	134.33
TiO ₂ with 0.5wt% CNMs	53.07 ± 0.5163	0.4569	253.51

Table S4: Comparison of PCE of DSSCs reported employing graphene/reduced graphene oxide-TiO₂ composite semiconductor photoanode

Photoanode Material	Synthesis/electrode fabrication method	Photoanode structure	Electrolyte	PCE/%	Ref.
TiO ₂ -GQDs	Hydrothermal/doctor blade	FTO/TiCl ₄ /TiO ₂ -GQDs/N719/(I ⁻ /I ₃ ⁻)/Pt	0.05 mM LiI, 0.03 mM I ₂ , 1.0MPMII	6.10	1
TiO ₂ -rGO	Hummers method/doctor blade	FTO/TiCl ₄ /TiO ₂ -GO/N719/(I ⁻ /I ₃ ⁻)/Pt	Commercial I ⁻ /I ₃ ⁻ , CH ₃ CN-Iodolyte AN-50	6.61	2
TiO ₂ -Graphene nanocomposite	Hydrothermal/doctor blade	FTO/TiCl ₄ /TiO ₂ -GO sheets/N719/(I ⁻ /I ₃ ⁻)/Pt	50mM LiI, 30 mM I ₂ , 0.5 M t-butyl pyridine, CH ₃ CN-Valeronitrile	7.1	3
Anatase TiO ₂ -RGO	Hydrothermal/doctor blade	FTO/TiCl ₄ /TiO ₂ -GO decorated/N719/(I ⁻ /I ₃ ⁻)/Pt	0.5 M LiI, 0.05 mM I ₂ , 0.2 M t-butyl pyridine, CH ₃ CN	7.68	4
TiO ₂ -CNMs	Hydrothermal/doctor blade	FTO/TiCl ₄ /TiO ₂ -CNMs/N719/(I ⁻ /I ₃ ⁻)/Pt	0.1 M LiI, 0.05 M I ₂ , 0.5 M t-butylpyridineand 0.6 M 1-butyl-3-methyl imidazolium iodide, 15% of valeronitrile and 85%acetonitrile	10.24	This work

- 1 X. Fang, M. Li, K. Guo, J. Li, M. P. Li hua, B. M.Luoshan and X.Z. Zhao, *Electrochim. Acta*,2014, **137**, 634-638.
- 2 R. Ramamoorthy, V. Eswaramoorthi, M. Sundararajan, M. Boobalan, A. D. Sivagamiand and R. Victor Williams, *J. Mater. Sci. Mater. El.*,2019, **30**, 12966–12980.
- 3 D. Wang, X. Wang, Y. Guo, W. Liu, W. Qin, *RScAdv.*,2014, **4**, 51658–51665.
- 4 G. Cheng, M. S. Akhtar, O. B. Yang and F. J. Stadler, *ACS Appl. Mater. Interfaces*,2013,**5**, 6635-6642.

Table S5: Values of passive elements obtained fitting Nyquist plots using R_s (R_1Q_1) (R_2Q_2) Randles circuit. Electrochemical Impedance parameters of (0, 0.5 and 1 wt.% variation photoanodes) with contact resistance (R_s), charge transfer resistance (R_1), admittance (Y_1), CPE index (n_1), derived from Y_1 and n_1 associated with the counter electrode; charge transfer resistance (R_2) admittance (Y_2), CPE index (n_2), capacitance (C_2) associated at photoanode-electrolyte interface, electron life time (τ_n), electron transport time (τ_s), and charge collection efficiency (η_{CC}).

Wt. % of CNMs	χ^2	$R_s(\Omega)/$ %Error	$R_1(\Omega)/$ %Error	$Y_1 (\mu\text{mho} \times \text{s}^n)/$ %Error	$n_1/$ % Error	$R_2(\Omega)/$ %Error	$Y_2 (\mu\text{mho} \times \text{s}^n)/$ %Error	$n_2/$ % Error	$C_2 (\mu\text{F})/$ % Error	$\tau_n (\text{ms})/$ % Error	$\tau_s (\text{ms})/$ % Error	$\eta_{CC} /$ % Error
0	3.59×10^{-4}	13.72/ 0.74	6.99/ 4.92	111/ 30.57	0.795/ 4.26	39.03/ 1.95	1180/ 5.12	0.856/ 1.69	705/ 12.38	27.52/ 14.33	9.67/ 13.12	0.739/ 0.31
0.5	1.56×10^{-4}	14.96/ 0.60	4.76/ 4.48	149/ 31.91	0.754/ 4.56	20.45/ 1.75	2060/ 4.77	0.851/ 1.59	1180/ 11.84	24.14/ 13.58	17.66/ 12.44	0.578/ 0.48
1	2.26×10^{-4}	18.87/ 0.77	5.15/ 7.17	256/ 46.30	0.703/ 7.22	23.46/ 2.11	2010/ 5.43	0.842/ 1.99	1132/ 14.09	26.55/ 16.20	21.36/ 14.86	0.554/ 0.60

Table S5 presents fitting parameters obtained from Nyquist plot where R_s , R_1 , and R_2 denote the contact and solution resistance, charge transfer resistance at Pt counter electrode-electrolyte interface, and the photoanode-electrolyte interface (back electron transfer) respectively. Q_1 and Q_2 are the constant phase element (CPE), which is a function of two parameters: Y (mho.sⁿ) and the CPE exponent n . The impedance of simple faradaic reaction

$$Z = \frac{R}{1 + (jW)^n Y R}$$

(without including diffusion) can be expressed in terms of a CPE as $1 + (jW)^n Y R$. The parameters n and Y are independent of frequency. When $n = 1$, Y has the units of capacitance i.e. (F or mho s⁻¹) and denotes the capacity of the interface and for $n \neq 1$, Y develops a unit of mho.sⁿ and the system shows behaviour that has been attributed to continuous distribution of time constants for the reaction occurring at the photoanode-electrolyte interface. The fitting was performed, neglecting the last few points that are drifting in the low-frequency region using ZsimWin 3.6 software. Table 3 includes goodness of fit (χ^2), CPE (Y_2 , [Mho.s^{n₂}]), and the CPE exponent (n_2) correspond to the photoanode-electrolyte interface. χ^2 is defined in equation 1. The equivalent capacitance of C_2 (pseudo-capacitance, C_2) was calculated using equation 2.

$$\chi_{elements}^2 = \sum_{i=low\ frequency}^{high\ frequency} \left(\frac{(O_i - E_i)^2}{E_i} \right) \quad (1)$$

$$C_2 = Y_2^{1/n_2} R_2^{\left(\frac{1}{n_2} - 1\right)} \quad (2)$$

where, O and E are observed, and expected values respectively for the elements belong to solution resistance (R_s), counter electrode impedance (R_1 , Y_1 and n_1) and photoanode impedance (R_2 , Y_2 , and n_2), at each frequency. The error in pseudo-capacitance C_2 was calculated differentiating equation 2 with respect to Y_2 , R_2 , and n_2 (equation 3-5).

$$\delta C_2 = \frac{\partial C_2}{\partial Y_2} \delta Y_2 + \frac{\partial C_2}{\partial R_2} \delta R_2 + \frac{\partial C_2}{\partial n_2} \delta n_2 \quad (3)$$

$$\begin{aligned} |\delta C_2| &= \left| \frac{\partial C_2}{\partial Y_2} \delta Y_2 + \frac{\partial C_2}{\partial R_2} \delta R_2 + \frac{\partial C_2}{\partial n_2} \delta n_2 \right| \\ &= \left| Y_2^{\left(\frac{1}{n_2} - 1\right)} R_2^{\left(\frac{1}{n_2} - 1\right)} \left(\frac{1}{n_2} \right) \right| |\delta Y_2| + \left| Y_2^{1/n_2} R_2^{\left(\frac{1}{n_2} - 2\right)} \left(\frac{1}{n_2} - 1 \right) \right| |\delta R_2| + \left| Y_2^{1/n_2} R_2^{\left(\frac{1}{n_2} - 1\right)} \right| |\delta n_2| \end{aligned} \quad (4)$$

Equation 5 was obtained substituting equation 2 into equation 4,

$$|\delta C_2| = \left(\frac{C_2}{n_2 Y_2} \right) |\delta Y_2| + \left(\frac{C_2}{R_2 n_2} \left(\frac{1}{n_2} - 1 \right) \right) |\delta R_2| - \frac{C_2}{n_2^2} (\ln Y_2 + \ln R_2) |\delta n_2| \quad (5)$$

where $|\delta C_2|$, $|\delta R_2|$, $|\delta Y_2|$ and $|\delta n_2|$ are absolute error in C_2 , R_2 , Y_2 , and n_2 respectively.

The lifetime (τ_n) and transport time (τ_s) of electron also calculated from the EIS data. These are two characteristic parameters required to explain the higher efficiency of DSSC over other. The lifetime is the important quantity which provides insight into the exciton recombination property of DSSC. Lifetime is the product of C_2 and R_2 and similarly, transport time is the product of R_S and C_2 .

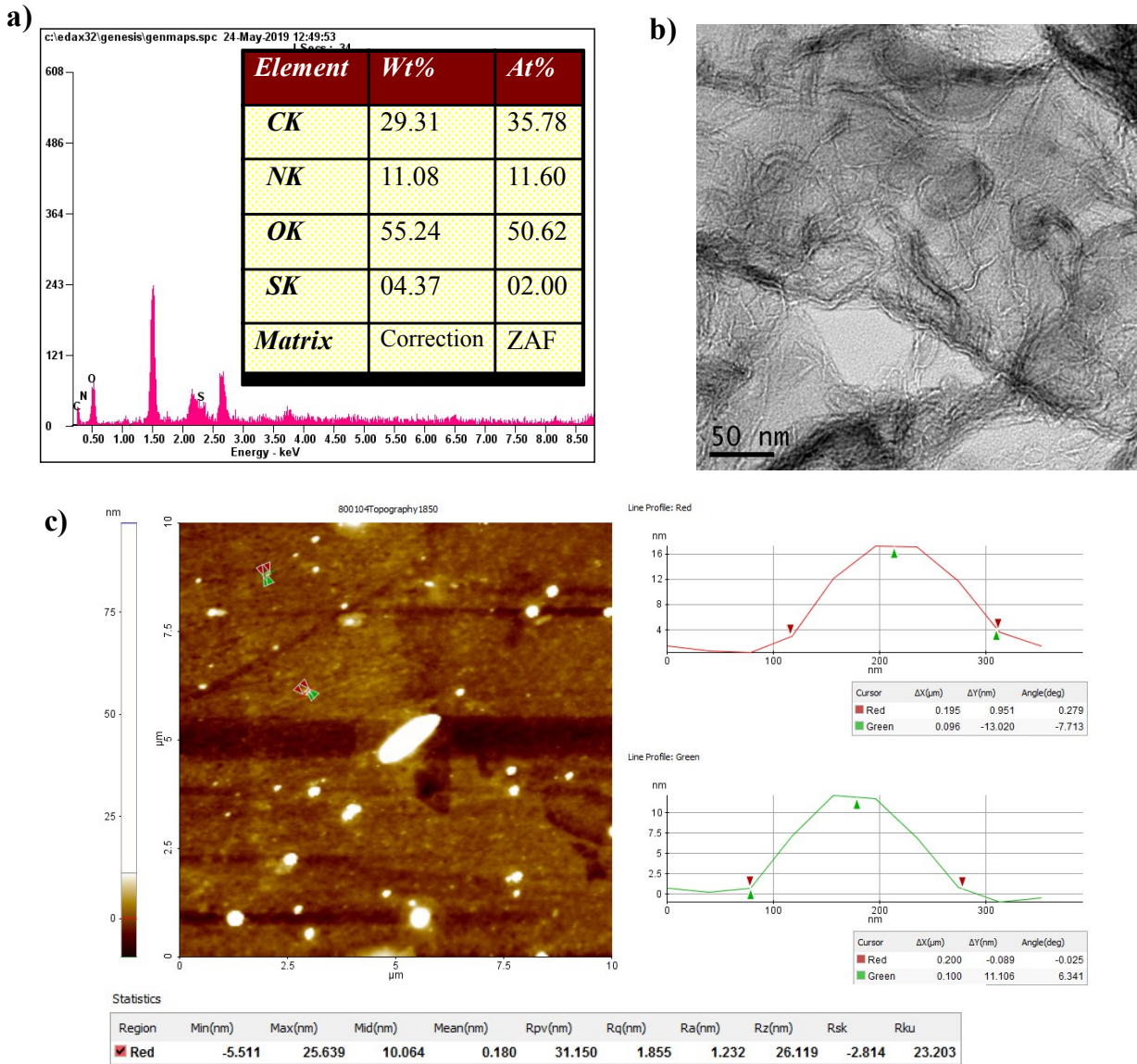


Figure S1: a) EDAX from HR-SEM b) HR-TEM image at 50 nm scale c) AFM image of CNMs.

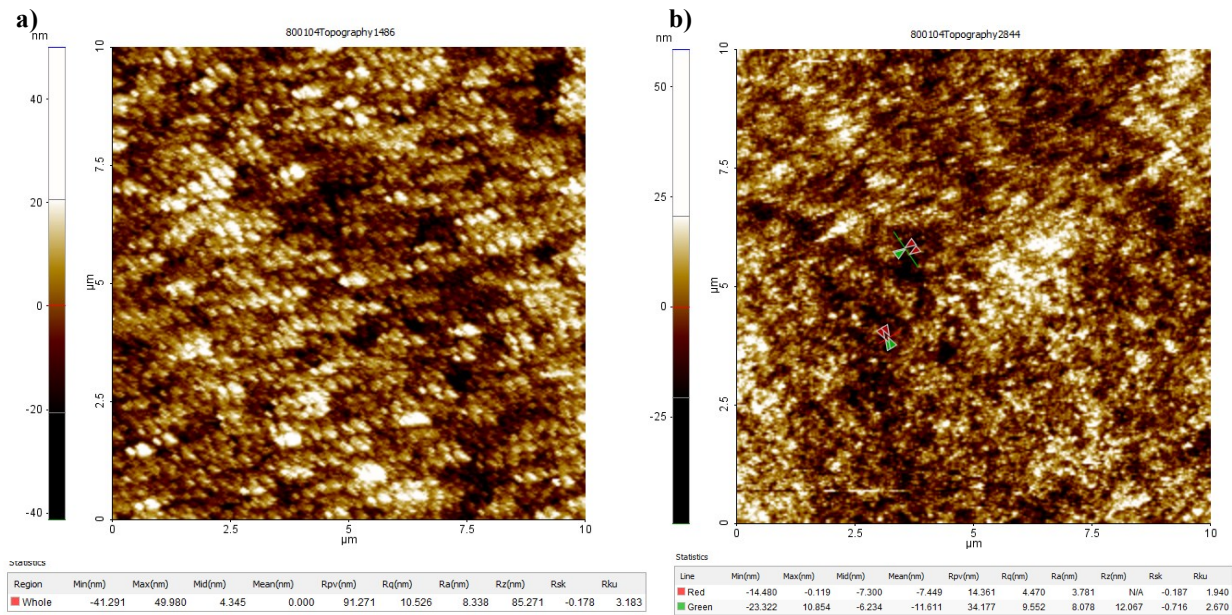


Figure S2: AFM analysis of a) transparent TiO₂ film and b) TiO₂ film loaded with 0.5 wt.% CNMs

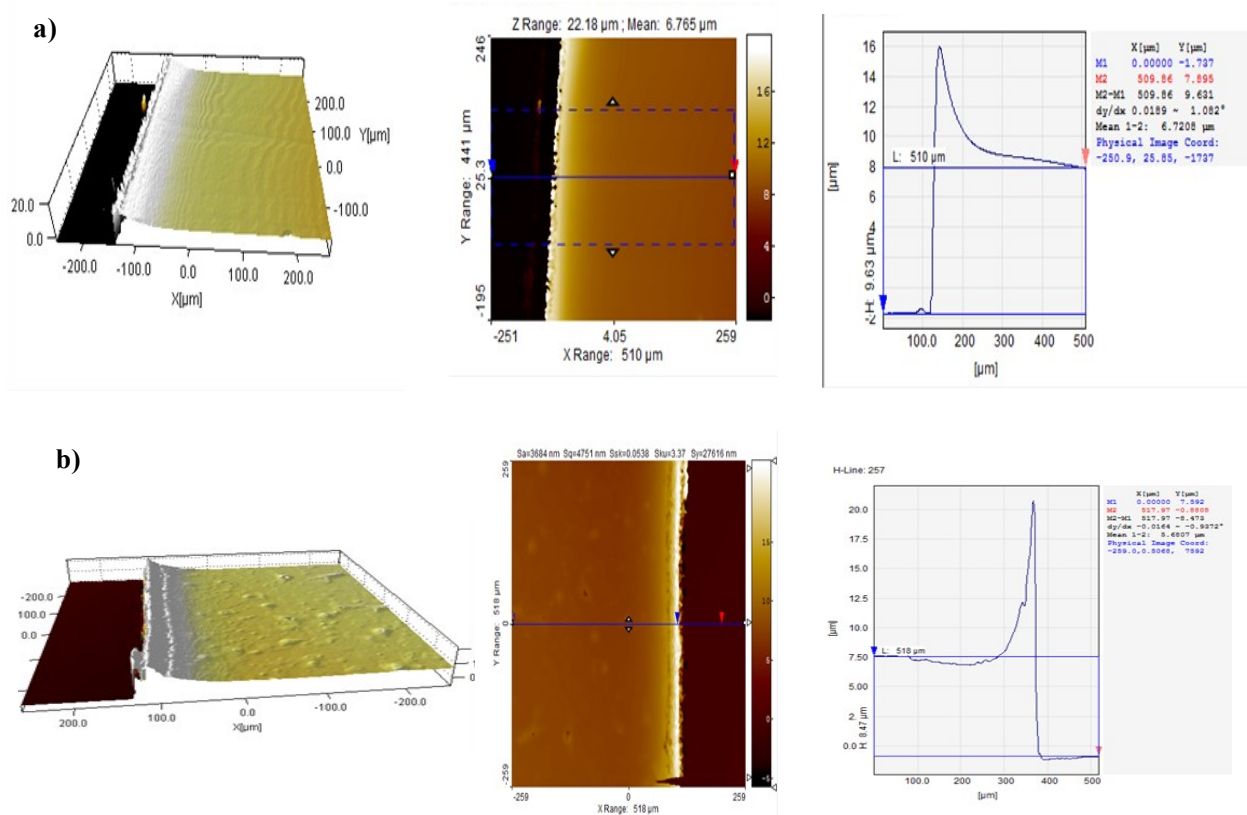


Figure S3: Profilometry analysis of a) transparent TiO_2 film and b) TiO_2 film loaded with 0.5 wt.% CNMs

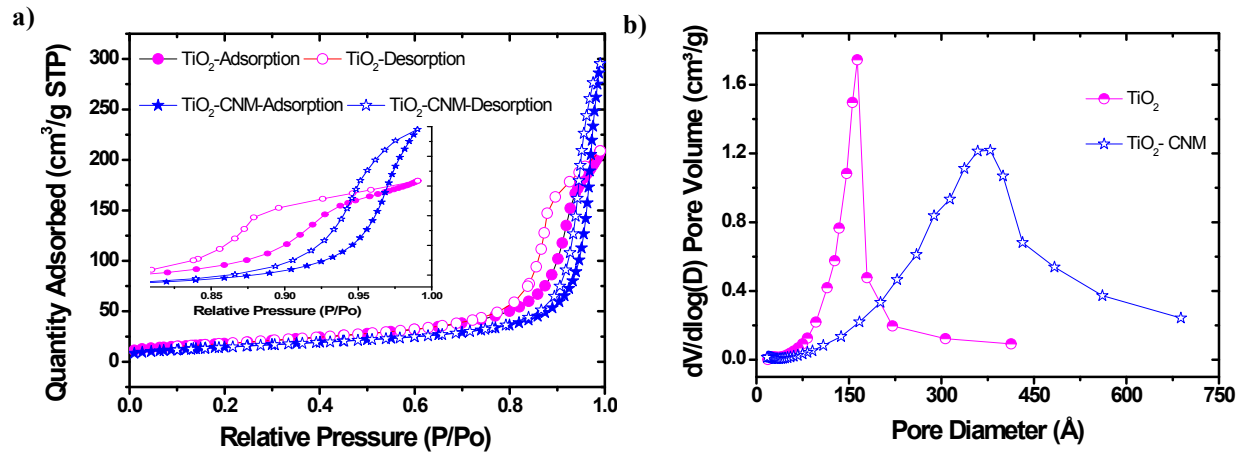


Figure S4: a) Isotherm linear plot and b) BJH pore size distribution analysis of TiO₂ and TiO₂ loaded with 0.5 wt.% of CNM.

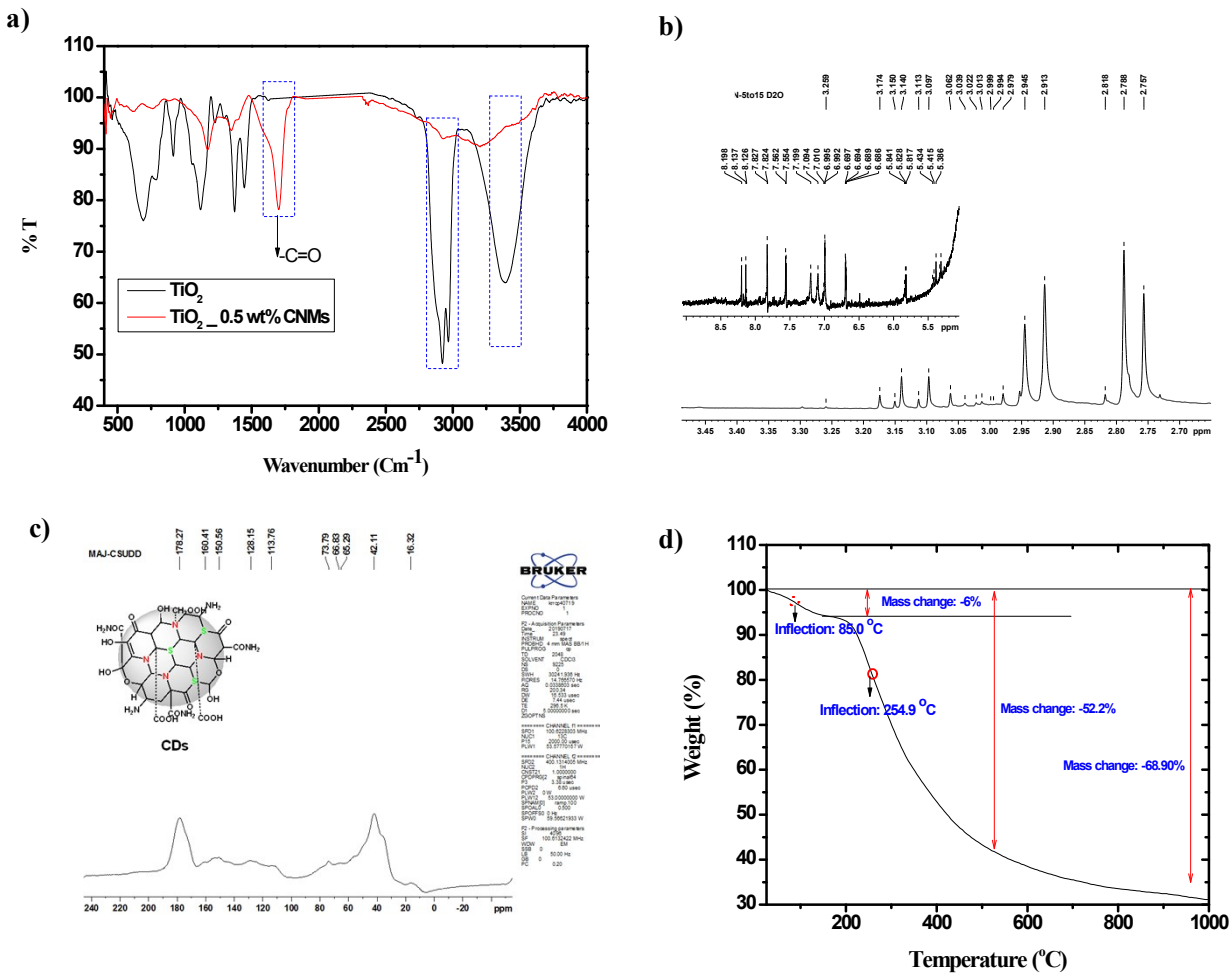


Figure S5: a) FT-IR, b) ^1H NMR, c) ^{13}C NMR and d) TGA analysis of CNMs

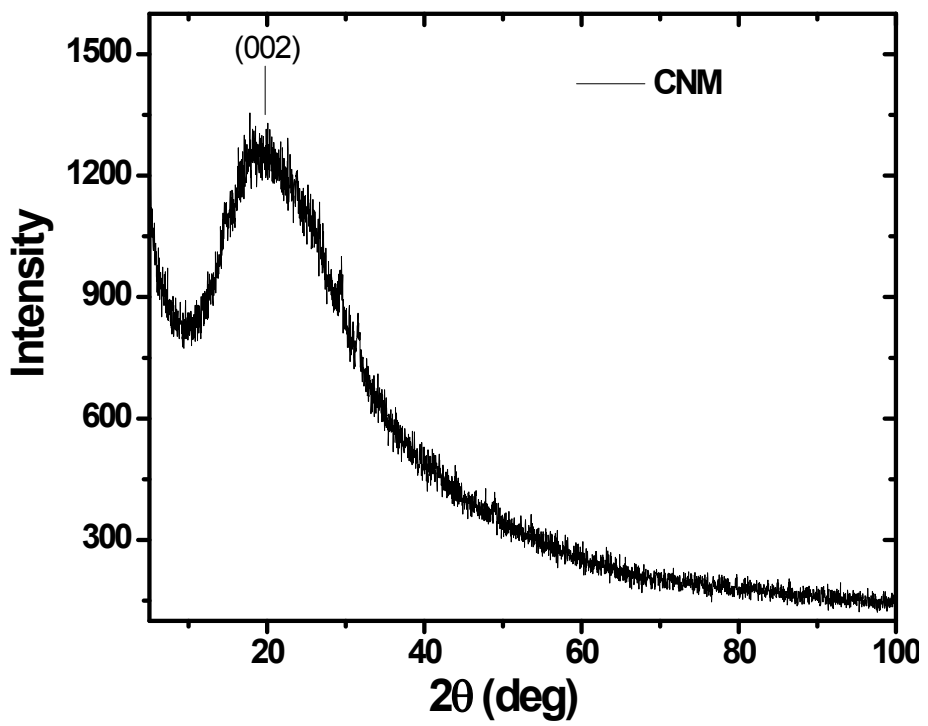


Figure S6: Powder XRD pattern of CNMs.

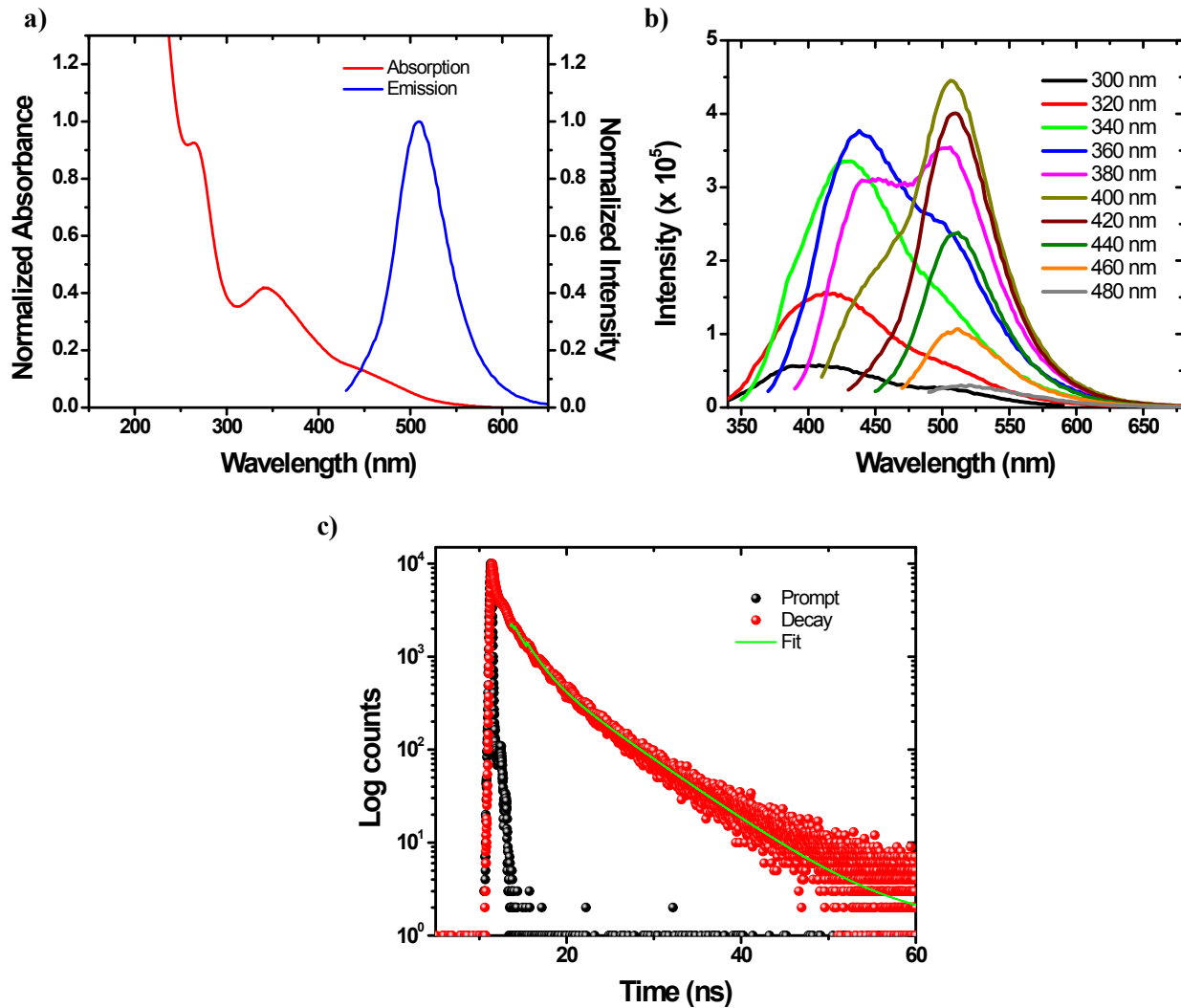


Figure S7: a) Absorption and emission spectra, b) Excitation dependent emission spectra and c) Fluorescence decay of CNMs.

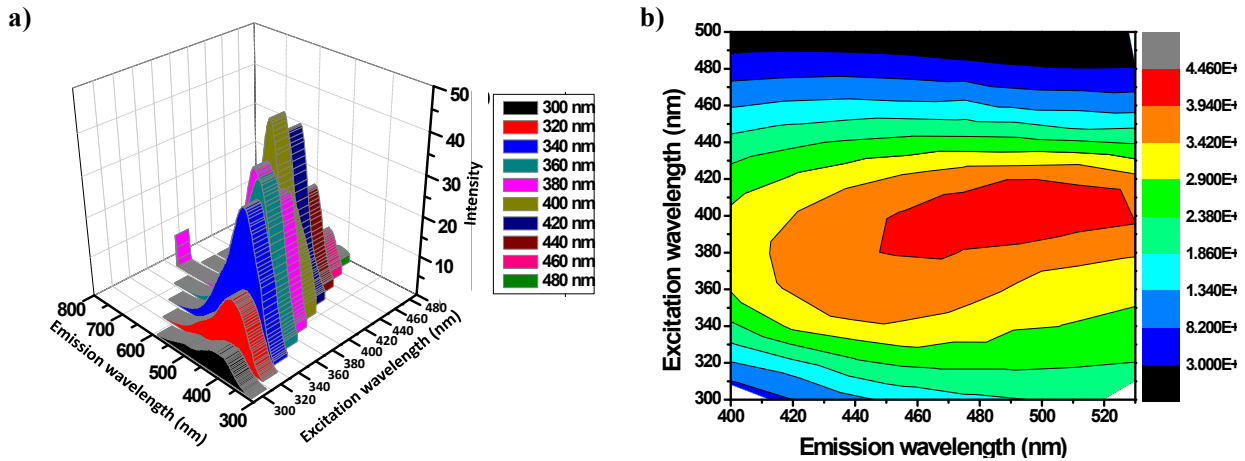


Figure S8: a) 3D excitation and emission plot b) color contour map of emission intensity of CNMs with different excitation.

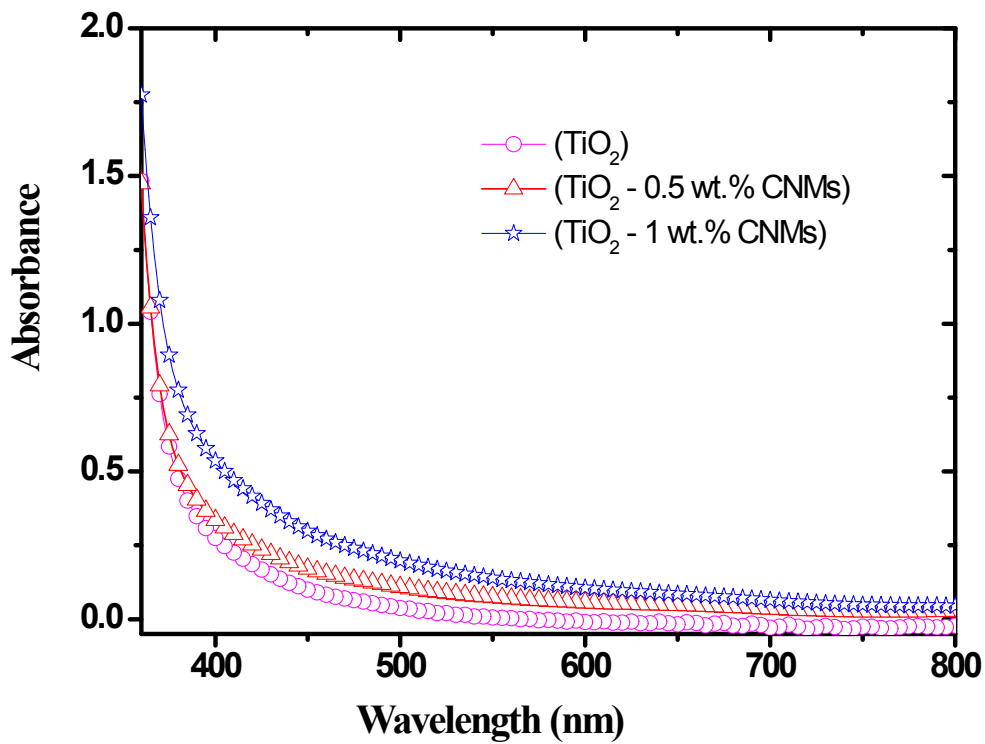


Figure S9: UV-Visible absorption spectra of TiO₂ with different wt.% (0, 0.5 and 1) loaded CNMs.

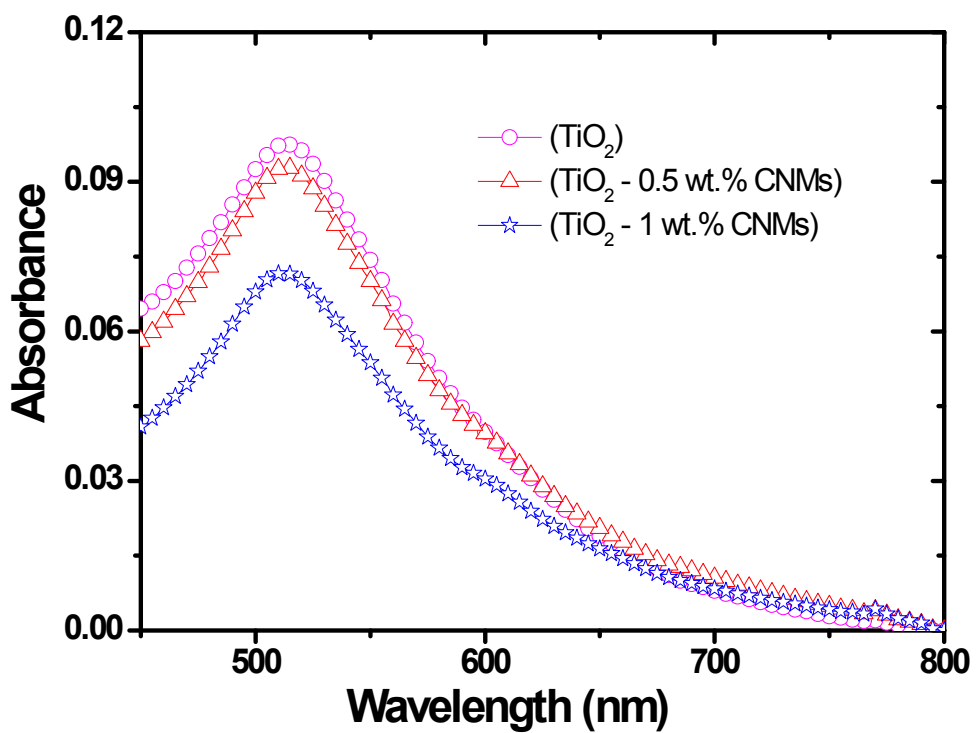


Figure S10: Dye loading of study of TiO_2 with different wt.% (0,0.5 and 1) loaded CNMs via UV-Visible absorption spectroscopy.